



## Piezoelectric actuation of direct-write electrospun fibers

Juan Pu<sup>a,b,\*</sup>, Xiaojun Yan<sup>a,c</sup>, Yadong Jiang<sup>b</sup>, Chieh Chang<sup>a</sup>, Liwei Lin<sup>a</sup>

<sup>a</sup> Berkeley Sensor and Actuator Center, Department of Mechanical Engineering, University of California, Berkeley 94720, United States

<sup>b</sup> School of Opto-electronic Information, University of Electronic Science and Technology of China, Chengdu 610054, China

<sup>c</sup> School of Jet Propulsion, Beihang University, Beijing 100191, China

### ARTICLE INFO

#### Article history:

Received 17 June 2010

Received in revised form

13 September 2010

Accepted 24 September 2010

Available online 1 October 2010

#### Keywords:

Piezoelectricity

Actuator

Electrospinning

Poly (vinylidene fluoride) (PVDF)

### ABSTRACT

Piezoelectric actuation of doubly clamped, electrospun poly (vinylidene fluoride) (PVDF) fibers fabricated by a direct-write process has been demonstrated. Near-field electrospinning (NFES) has been utilized to fabricate PVDF fibers with good piezoelectric properties by means of the *in situ* electrical poling and mechanical stretching process. Experimentally, PVDF fibers have responded to both piezoelectric and electrostatic effects and a double-electrode approach has been used to minimize the electrostatic effect. An average piezoelectric coefficient  $d_{33}$  of  $-57.6$  pm/V has been characterized from fabricated fibers and this value is about twice larger than the value reported in PVDF thin-films. Various complex patterns of PVDF fibers have been deposited using NFES, enabling possible array formats for fiber-based actuators with possible applications including artificial muscles and switches.

© 2010 Elsevier B.V. All rights reserved.

### 1. Introduction

As a piezoelectric polymer, Poly (vinylidene fluoride) (PVDF) is attractive in energy conversion applications between electric and mechanical forms because of its low cost, high flexibility and biocompatibility. The piezoelectric property of (PVDF) has been utilized in various device applications, such as strain sensors [1–4], mechanical actuators [5–7], energy harvesters [8–11] and artificial muscles [12]. Recent advancements in nanotechnology have further explored the possibility of using PVDF nanofibers for possible applications in nano sensors, actuators and energy generators. The aforementioned applications rely on good piezoelectric property of PVDF and it is well-known that proper mechanical stretching and electrical poling are necessary to achieve good piezoelectricity. Electrospinning processes can construct PVDF fibers with simultaneous *in situ* mechanical stretch and electrical poling [13–16]. However, existing conventional electrospinning processes produce fibers that do not exhibit useful piezoelectric responses as a whole because piezoelectric reactions of randomly distributed fibers cancel out each other such that their overall piezoelectric outputs are negligible.

A direct-write electrospinning technique by means of near-field electrospinning (NFES) [17,18] has been developed to produce ori-

entation controllable depositions of fibers of various materials. Previously, Chang et al. have reported nanogenerators based on electrospun PVDF nanofibers [19] with high energy conversion efficiency for potential wearable ‘smart clothes’ to power hand-held electronics through body movements. Here, piezoelectric actuation characteristics of a single electrospun PVDF fiber are investigated for potential applications in actuators, switches and artificial muscles. Furthermore, controllability of electrospun PVDF fibers using NFES has been demonstrated for potential array formats of polymeric actuators.

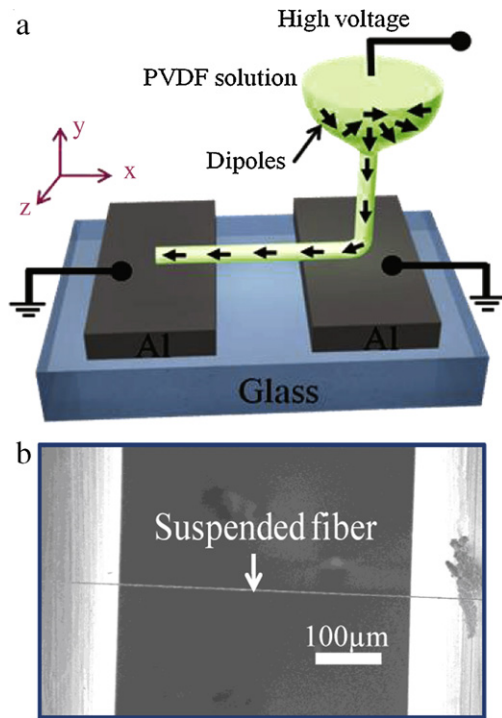
### 2. Design and fabrication

Fig. 1a illustrates the schematic diagram of a single, suspended fiber across two aluminum contact pads (made of  $81\ \mu\text{m}$ -thick aluminum foil) on an insulation glass substrate fabricated by the direct-write electrospinning process. Conductive epoxy was used to fix the two ends of the suspended fiber. The typical air gap between the two contacts is  $500\text{--}1000\ \mu\text{m}$  and the direct-write technique is realized by using an  $x$ - $y$  stage (Newport, Inc.) to control the deposition speed and direction of the glass substrate during the NFES process.

In the preparation of PVDF solution, dimethyl sulfoxide (DMSO) is used as solvent for PVDF powder ( $M_w = 534000$ ), with added acetone and fluorosurfactant (ZONYL® UR) to improve the evaporation rate and reduce the surface tension of the solution, respectively. Fig. 1b shows the SEM image of a fabricated PVDF fiber ( $2.6\ \mu\text{m}$  in diameter and  $500\ \mu\text{m}$  in length). The electrospinning process parameters used in this case are: 16 wt% PVDF, 80 wt% sol-

\* Corresponding author at: Berkeley Sensor and Actuator Center, Department of Mechanical Engineering, University of California, 1113 Etcheverry Hall, Berkeley 94720, United States. Tel.: +1 510 735 7685.

E-mail address: [pujuan2007@hotmail.com](mailto:pujuan2007@hotmail.com) (J. Pu).



**Fig. 1.** (a) Schematic diagram of the direct-write electrospinning process with *in situ* poling to construct suspended piezoelectric PVDF fiber. The polarity of the fiber is determined as shown. Conductive epoxy was added to fix the fibers on the aluminum contact electrodes. (b) SEM image of a suspended PVDF fiber with diameter of 2.6  $\mu\text{m}$  and length of 500  $\mu\text{m}$ . The fiber in (a) was enlarged for illustration purpose.

vent (DMSO:acetone with 1:1 weight ratio), 4 wt% fluorosurfactant (ZONYL<sup>®</sup> UR), 1 mm for the needle-to-collector distance, 1.1 kV for the electrospinning voltage, and 35 mm/s for the  $x$ - $y$  stage moving speed.

Under the applied electrical field, piezoelectric effect will generate mechanical strain with a magnitude  $\varepsilon_p$  along the fiber axis as (without considering external forces applied on the fiber):

$$\varepsilon_p = d_{33}E \quad (1)$$

where  $E$  is the applied electric field, and  $d_{33}$  is the piezoelectric coefficient. PVDF has negative  $d_{33}$  such that positive (in the same direction with the polarity of the fiber) and negative (in the direction opposite to the polarity) electric fields result in shrinkage and elongation of the fiber, respectively. Therefore, the piezoelectric responses of PVDF fiber with two ends fixed under an applied electric field can be characterized as following. (a) In the ideal case, the suspended fiber is straight without initial deformation. Under positive electric field, a tensile strain will be generated with no observable  $y$ -directional deformation since the fiber is fixed at its two ends. Under negative electric field, the fiber will buckle in any direction in the  $y$ - $z$  plane assuming the fiber has perfect circular cross section. (b) In reality, the suspended fiber has initial downward deformation (along the  $-y$  direction) which results from gravity force during the electrospinning process. The positive and negative electric field will reduce and increase the downward deformation, respectively. Furthermore, the “initial deformation” of the suspended fiber can be adjusted by changing the moving speed of the substrate during electrospinning process. Higher moving speed results in smaller initial deformation, even initial residual tensile strain, but fibers break easily if the substrate moving speed is higher than 90 mm/s. In the rest of the discussions throughout the paper, “deformation” is defined as the deflection at the center of the fiber relative to its initial deformation after the deposition process.

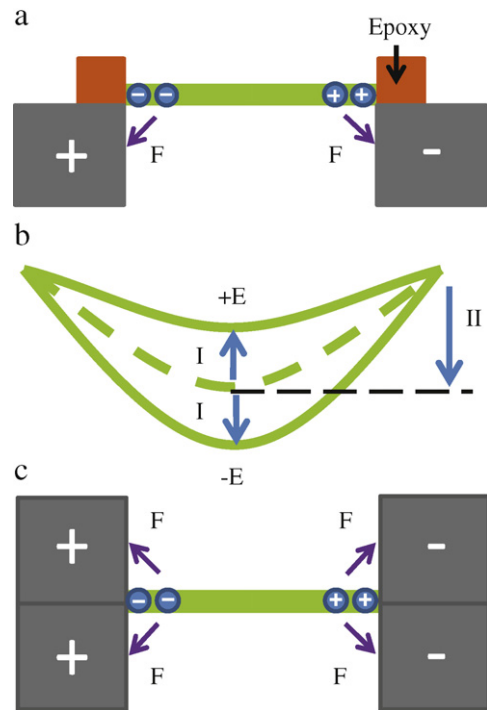


**Fig. 2.** (a) Side view diagram to illustrate the electrostatic attraction force. (b) Deformation of PVDF fiber under positive (+E) or negative (-E) electrical field as a result of both (I) piezoelectric and (II) electrostatic effects. (c) With additional top aluminum electrodes, the effects of electrostatic force can be reduced. The fibers in (a)–(c) were enlarged for illustration purpose.

Practically, electrostatic effect also contributes to the deformation of the fiber. Under an electrical bias as illustrated in Fig. 2a, charges in the fiber migrate to both ends with a built-in potential [20,21]. The electrostatic attraction force, either under positive or negative electrical field, deforms the fiber downwards as shown in Fig. 2b. When a positive electrical field is applied, the total deformation is equal to the combined downward electrostatic and upward piezoelectric deformation. When a negative electrical field is applied, the total deformation is equal to combined downward electrostatic and downward piezoelectric deformation. Analytically, electrostatic force comes mainly from the asymmetry of electrodes in the  $y$  direction as electrodes are only placed on the bottom of the fiber. Therefore, adding two extra electrodes on top of the two bottom aluminum electrodes could reduce the electrostatic effect as illustrated in Fig. 2c.

### 3. Simulation

The piezoelectric responses of a suspended PVDF fiber to the applied electric field along the  $x$ -direction are calculated using finite element method (FEM), as shown in Fig. 3a. In this case, the fiber has a diameter of 5  $\mu\text{m}$  and length of 1 mm and the material properties of bulk PVDF are adopted as: Young's modulus  $E = 2.5$  GP, Poisson's ratio  $\nu = 0.348$  [22], relative dielectric constants  $\kappa = 8$  [23], and piezoelectric constants  $d_{31} = 20$  pm/V,  $d_{32} = 3$  pm/V and  $d_{33} = -33$  pm/V [24]. In the simulation, the boundary conditions are set as followings: the two ends of the fiber are mechanically fixed (displacements in all directions are zero) and the other parts are free to move to a mechanical equilibrium state, and the voltage is applied along the  $x$ -axis. In the experiments, the fiber has initial downward deformation (in the  $-y$  direction) due to gravity during electrospinning process which can be adjusted by controlling the moving speed of the  $x$ - $y$  stage. Thus, in the simulation the initial downward deformation is taken into account by using

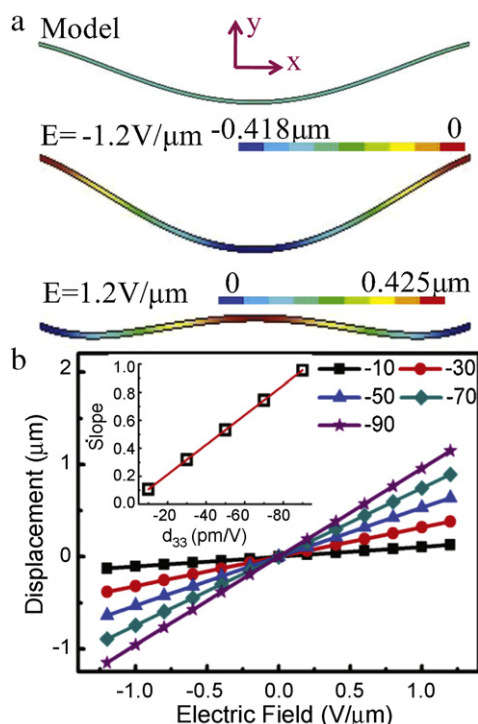


**Fig. 3.** (a) Simulation results illustrate the deformation of the fiber. (top) Initial deformation of 20 μm under gravity. (center) Deformation under applied electric fields of -1.2 V/μm along x-axis. (bottom) Deformation under 1.2 V/μm along x-axis. The deformations were enlarged for illustration purpose. (b) Piezoelectric simulation results showing the relationship between fiber central deformations with respect to applied electric field for different  $d_{33}$  varying from -10 to -90 pm/V. For each  $d_{33}$ , the simulation data was linearly fitted, so each linearly fitted line corresponds to a value of  $d_{33}$ . The inset shows the dependence of the slope of linearly fitted line on  $d_{33}$ .

a curving model (Fig. 3a) which has initial downward displacement of 20 μm at the center. Under an electric field of -1.2 and 1.2 V/μm, the center of the fiber has displacements relative to its initial downward deformation of -0.418 and 0.425 μm as a result of piezoelectric effect, respectively. Simulation results indicating the linear relationship between fiber central deformations and the applied electric fields of varying  $d_{33}$  from -10 to -90 pm/V are shown in Fig. 3b. The dependence of the linearly fitted line slope on  $d_{33}$  are plotted as the inset of Fig. 3b as the foundation to approximate  $d_{33}$  of the PVDF fiber fabricated in this work.

#### 4. Experimental results and discussions

The deformations at the fiber center are measured using a digital microscope with a charge-coupled device (CCD). An advanced image capture and processing software, “Infinity Analyze,” (by Lumenera Corporation) is used to characterize the displacements. During the experiments, the actuator is tilted 90° in order to observe and characterize the upward and downward movements at the center of the fiber. Before the experiments, the image of a fabricated microstructure with circular dots is captured for calibration, as shown in Fig. 4a. Center-to-center distance of two neighboring dots in the same row or column is 8 μm and the calibration process is conducted by placing a line on the image and specifying the length between the centers of two dots with known distance. Fig. 4b illustrates that the fiber center has a displacement of  $-1.57 \pm 0.2 \mu\text{m}$  under an applied electric field of -1.2 V/μm. The measurement uncertainty mainly comes from the determinations of the edges of the fiber on the images.

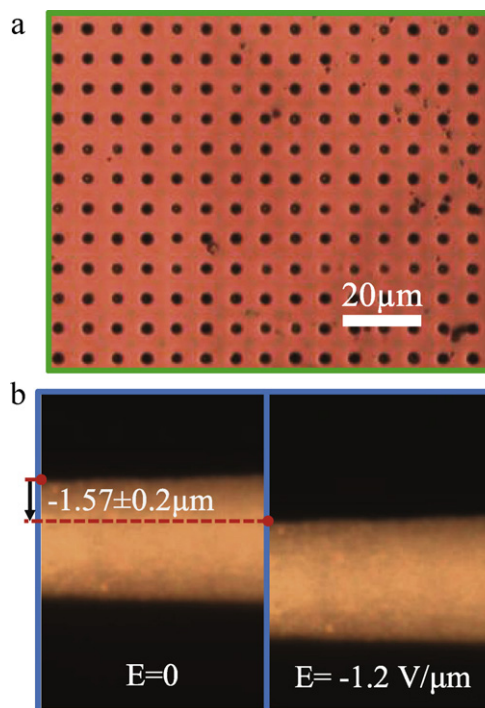


**Fig. 4.** (a) A micro device with known geometry is used for calibration. (b) Optical images of the fiber center positions before and after the applied electric field of -1.2 V/μm.

Fig. 5a and b shows measured central deformations (relative to the initial downward deformation of 20 μm) of an electrospun fiber under positive and negative electrical fields with one-layer and double-layer electrodes, respectively (the second aluminum

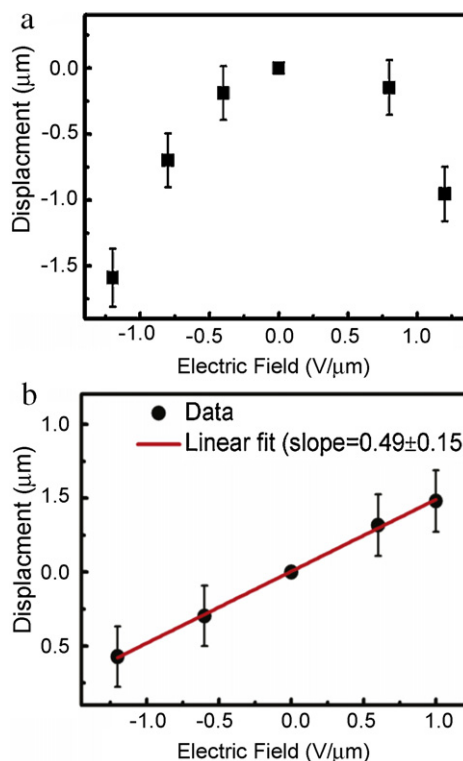


**Fig. 5.** Experimental results showing the fiber central deformations corresponding to different electric fields with (a) one-layer and (b) double-layer electrodes, respectively.

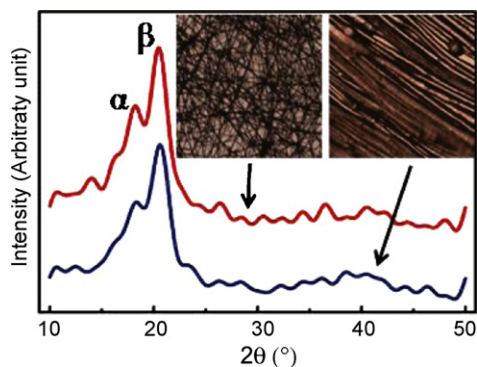


Fig. 6. XRD diffraction patterns of the randomly and orderly aligned PVDF fibers fabricated by conventional and NFES processes, respectively.

electrode is glued on top of the first electrode). Results from the one-layer electrode setup in Fig. 5a show downward displacements along the  $y$  direction at the center of the fiber for both positive and negative electric fields. This implies that the electrostatic force contributes significantly to the measured data. Theoretically, the existence of piezoelectric effect should cause larger downward displacements under negative electric field as compared with the displacements under positive electric field and this phenomenon is observed as illustrated. By constructing the double-layer electric electrodes, the electrostatic effect is minimized as illustrated in Fig. 5b. The downward deformations are reduced under the negative electric fields and the upward deformations are observed under positive electric fields. This indicates the electrostatic effect has been minimized and the piezoelectric actuation dominates the total effects. According to the linear fit of the measured data,  $d_{33}$  is estimated to be  $46 \pm 14$  pm/V based on the simulations results in Fig. 3b.

PVDF is a semicrystalline polymer that consists of four crystalline phases of  $\alpha$ ,  $\beta$ ,  $\gamma$  and  $\delta$ . Among these, non-polar  $\alpha$  phase is the most common phase and is usually found in commercially available powders and films. It has random orientation of dipole moments with poor piezoelectricity.  $\beta$  phase has all the dipole moments pointing to the same direction and it is responsible for the piezoelectric responses of PVDF. In order to verify the *in situ* electric poling and mechanical stretching effects during the NFES process, XRD (X-ray Diffraction) patterns of randomly and orderly, as-electrospun PVDF fibers are characterized as shown in Fig. 6, respectively. In both cases, a dominant peak at  $2\theta = 20.6^\circ$  corresponds to 200/110 reflections of the  $\beta$  phase. This implies that the high electric field during the electrospinning process aligns the dipole moments and produces good piezoelectric materials. Therefore, electrospinning of PVDF from its solution can transform non-polar  $\alpha$  phase in the crystalline into polar  $\beta$  phase and introduce the piezoelectric effect of electrospun PVDF fibers.

Fig. 7 shows that in comparison with commercially available PVDF thin films [25–29], the electrospun PVDF fibers with diameters ranging from 1 to 5  $\mu\text{m}$  have higher piezoelectric coefficients  $d_{33}$ , which exhibit an average value of  $-57.6$  pm/V based on 6 samples. Several possible reasons could have contributed to the enhanced piezoelectric properties. For example, PVDF fibers deposited by the NFES process could have fewer defects than the PVDF thin film due to a higher degree of crystallinity and chain orientation [19]. Furthermore, significant fraction of the piezoelectric responses could come from extrinsic effects collectively known as “domain wall motion” [30]. Compared with PVDF thin film, much smaller domain wall motion barrier in PVDF fibers was identified which results in large piezoelectric responses [19].

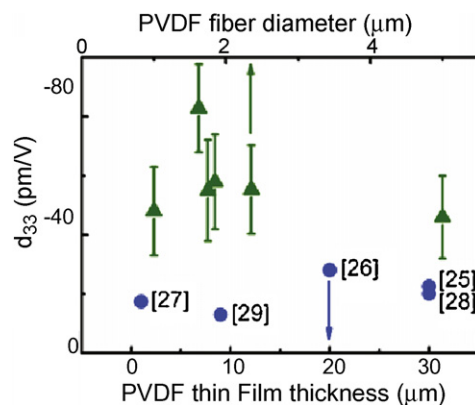


Fig. 7. Comparison between measured  $d_{33}$  of electrospun PVDF fibers (triangular dots) and reported  $d_{33}$  of PVDF thin film (circular dots) with different feature size.

## 5. Controllability of NEFS

Control capability of electrospinning is a key issue to make functional devices and to tailor their performance. During NEFS, the diameters of fibers could be controlled by adjusting various electrospinning parameters, such as PVDF concentration, electrospinning voltage, needle-to-collector distance and  $x$ - $y$  stage moving speed. Fig. 8a and b shows the controllability of fiber diameters based on needle-to-collector distance and  $x$ - $y$  stage moving speed, respectively. Increasing the stage moving speed could produce thinner PVDF fibers, as shown in Fig. 8a. However, higher speed (more than 90 mm/s) would terminate the electrospinning process, making fiber discontinuous. Experimental result in Fig. 8b shows the

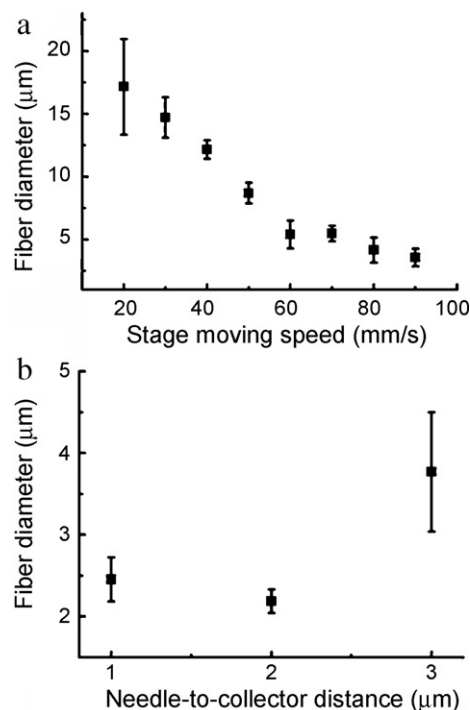
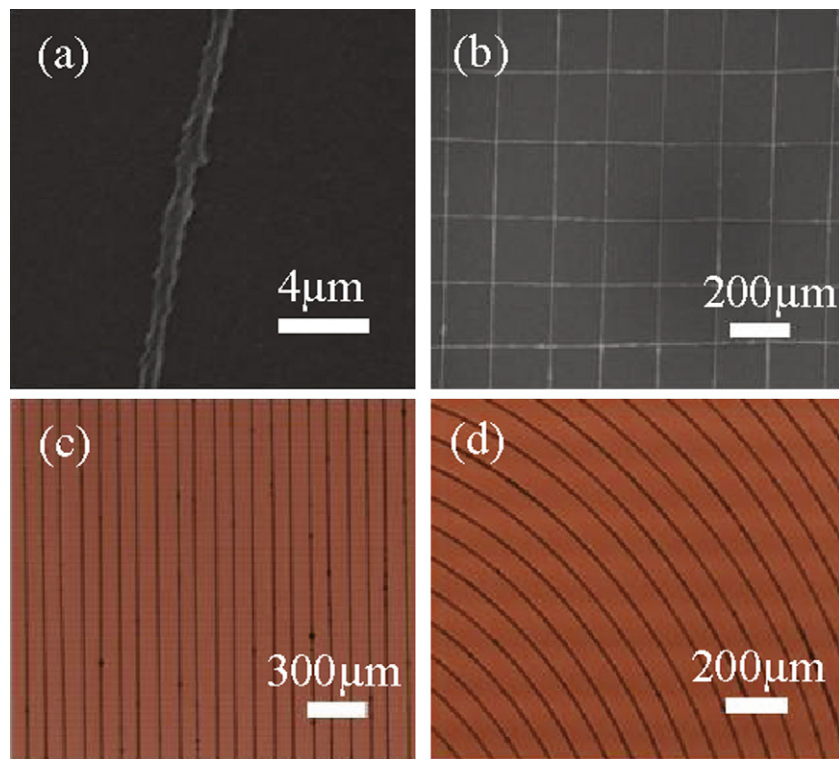


Fig. 8. Dependence of electrospun PVDF fiber diameters on the electrospinning parameters. (a) Stage moving speed. Other parameters are as follows: 16 wt% PVDF, 80% solvent (DMSO: acetone with 1:1 weight ratio), 4 wt% fluorosurfactant (ZONYL® UR), 1.5 mm for the needle-to-collector distance and 0.92 kV for the electrospinning voltage. (b) Needle-to-collector distance. Other parameters are as follows: 16 wt% PVDF, 80% solvent (DMSO: acetone with 1:1 weight ratio), 4 wt% fluorosurfactant (ZONYL® UR), 40 mm/s for the stage moving speed and 1 kV for the electrospinning voltage.



**Fig. 9.** Experiments showing controllability of NEFS for PVDF fibers. (a) A single electrospun PVDF nanofiber with diameter of 550 nm. (b) A grid pattern with controlled 200  $\mu\text{m}$  spacing. (c) Parallel fibers with controlled 100  $\mu\text{m}$  spacing. (d) Arc pattern with controlled 100  $\mu\text{m}$  spacing.

relationship between fiber diameter and needle-to-collector distance. When the needle-to-collector distance is increased from 1 to 2 mm, the PVDF fiber diameter is decreased because of the lower electric field for NFES (larger needle-to-collector distance while the voltage remains the same) results in smaller polymeric jet emerging from the cone, thus reducing the diameters of electrospun fibers [19]. However, when the needle-to-collector distance is increased from 2 to 3 mm, the fiber diameter is increased dramatically. This is believed that the formation of fiber has changed from near-field electrospinning to the conventional electrospinning process. In the conventional electrospinning process, smaller electrical field results in smaller stretching force [31] and fibers with larger diameters. Further investigations will be required to systematically characterize this transition region and provide design guidelines for the control of both the near-field and conventional electrospinning processes.

Furthermore, NEFS has the capability to control the deposition position of PVDF fibers in contrast to random deposition by conventional electrospinning processes. In our demonstrations, the PVDF fiber with a diameter of 550 nm is deposited continuously and the complex patterns are assembled by controlling the movement of the collector using a programmable  $x$ - $y$  stage (Newport, Inc), shown in Fig. 9a–d. This enables possible applications of actuators in the array format for larger force and/or deformation applications based on electrospun fibers.

## 6. Conclusions

In summary, piezoelectric response of a suspended PVDF fiber directly written by NFES has been characterized. The double-electrode setup significantly reduces the effects of electrostatic force such that it is possible to characterize the piezoelectric effects of electrospun fibers systematically. It is found that electrospun PVDF fibers have larger (about twice) piezoelectric coefficient  $d_{33}$  than that of PVDF thin films possibly due to fewer defects and

smaller domain wall motion barrier in PVDF fibers. Moreover, controllability of electrospun PVDF fibers using NEFS has been demonstrated for possible array fabrication. We believe that actuators made by electrospun PVDF fiber could enable various potential actuation applications for NEMS/MEMS.

## Acknowledgements

The authors would like to acknowledge Xiaojun Zhang for the help of XRD measurement. This project is supported in part by NSF grants 0901864 and 0832819.

## References

- [1] S. Choi, Z. Jiang, A novel wearable sensor device with conductive fabric and PVDF film for monitoring cardiorespiratory signals, *Sens. Actuators A: Phys.* 128 (2006) 317–326.
- [2] M. Toda, J. Dahl, PVDF corrugated transducer for ultrasonic ranging sensor, *Sens. Actuators A: Phys.* 134 (2007) 427–435.
- [3] L. Yang, C. Hsu, J. Ho, C. Feng, Flapping wings with PVDF sensors to modify the aerodynamic forces of a micro aerial vehicle, *Sens. Actuators A: Phys.* 139 (2007) 95–103.
- [4] Z. Chen, K. Kwon, X. Tan, Integrated IPMC/PVDF sensory actuator and its validation in feedback control, *Sens. Actuators A: Phys.* 144 (2008) 231–241.
- [5] C.S. Lee, J. Joo, S. Han, S.K. Koh, An approach to durable PVDF cantilevers with highly conducting PEDOT/PSS (DMSO) electrodes, *Sens. Actuators A: Phys.* 121 (2005) 373–381.
- [6] R.S. Wiederkehr, M.C. Salvadori, J. Brugger, F.T. Degasperi, M. Cattani, The gas flow rate increase obtained by an oscillating piezoelectric actuator on a micronozzle, *Sens. Actuators A: Phys.* 144 (2008) 154–160.
- [7] N. Snis, E. Edqvist, U. Simu, S. Johansson, Monolithic fabrication of multilayer P(VDF-TrFE) cantilevers, *Sens. Actuators A: Phys.* 144 (2008) 314–320.
- [8] N.S. Shenck, J.A. Paradiso, Energy scavenging with shoe-mounted piezoelectrics, *IEEE Micro*, 21 (2001) 30–42.
- [9] J. Granstorm, J. Feenstra, H.A. Sodano, K. Farinholt, Energy harvesting from a backpack instrumented with piezoelectric shoulder straps, *Smart Mater. Struct.* 16 (2007) 1810–1820.
- [10] L. Wu, L. Chen, C. Liu, Acoustic energy harvesting using resonant cavity of a sonic crystal, *Appl. Phys. Lett.* 95 (2009) 013506.
- [11] D. Wang, H. Ko, Piezoelectric energy harvesting from flow-induced vibration, *J. Micromech. Microeng.* 20 (2010) 025019.

- [12] M. Shahinpoor, Artificial muscles, *Encyclo. Biomater. Biomed. Eng.* 1 (1) (2004) 43–52.
- [13] W.A. Yee, M. Kotaki, Y. Liu, X. Lu, Morphology, polymorphism behavior and molecular orientation of electrospun poly(vinylidene fluoride) fibers, *Polymer* 48 (2007) 512–521.
- [14] Z. Zhao, J. Li, X. Yuan, X. Li, Y. Zhang, J. Sheng, Preparation and properties of electrospun poly(vinylidene fluoride) membranes, *J. Appl. Polym. Sci.* 97 (2005) 466–474.
- [15] X. Ren, Y. Dzenis, Novel continuous poly(vinylidene fluoride) nanofibers, *Mater. Res. Soc. Symp. Proc.* 920 (2006) 55–61.
- [16] S. Huang, W.A. Yee, W.C. Tjiu, Y. Liu, M. Kotaki, Y.C.F. Boey, J. Ma, T. Liu, X. Lu, Electrospinning of polyvinylidene difluoride with carbon nanotubes: synergistic effects of extensional force and interfacial interaction on crystalline structures, *Langmuir* 24 (2008) 13621–13626.
- [17] D. Sun, C. Chang, S. Li, L. Lin, Near-field electrospinning, *Nanoletters* 6 (2006) 839–842.
- [18] C. Chang, K. Limkrajaisiri, L. Lin, Continuous near-field electrospinning for large area deposition of orderly nanofiber patterns, *Appl. Phys. Lett.* 93 (2008) 123111.
- [19] C. Chang, V.H. Tran, J. Wang, Y. Fuh, L. Lin, Direct-write piezoelectric polymeric nanogenerator with high energy conversion efficiency, *Nanoletters* 10 (2010) 726–731.
- [20] E.R. Neagu, J.S. Hornsby, D.K. Das-Gupta, Polarization and space charge analysis in thermally poled PVDF, *J. Phys. D: Appl. Phys.* 35 (2002) 1229–1235.
- [21] W. Eisenmenger, H. Schmidt, B. Dehnen, Space charge and dipoles in polyvinylidene fluoride, *Braz. J. Phys.* 29 (1999) 295–305.
- [22] A. Vinogradov, F. Holloway, Electro-mechanical properties of the piezoelectric polymer PVDF, *Ferroelectrics* 226 (1999) 169–181.
- [23] Y. Higashihata, J. Sako, T. Yagi, Piezoelectricity of vinylidene fluoride-trifluoroethylene copolymers, *Ferroelectrics* 32 (1981) 85–92.
- [24] I. Chopra, Review of state of art of smart structures and integrated systems, *AIAA J.* 40 (2002) 2145–2187.
- [25] T.R. Dargaville, M. Celina, P.M. Chaplya, Evaluation of piezoelectric PVDF polymers for use in space environments. Part I. Temperature limitations, *J. Polym. Sci. B: Polym. Phys.* 43 (2005) 1310–1320.
- [26] Y. Ye, Y. Jiang, Zh. Wu, H. Zeng, Phase transitions of poly(vinylidene fluoride) under electric fields, *Integr. Ferroelectr.* 80 (2006) 245–251.
- [27] X. He, K. Yao, Crystallization mechanism and piezoelectric properties of solution-derived ferroelectric poly(vinylidene fluoride) thin films, *Appl. Phys. Lett.* 89 (2006) 112909.
- [28] M.C. Celina, T.R. Dargaville, P.M. Chaplya, R.L. Clough, Piezoelectric PVDF materials performance and operation limits in space environments, *Mater. Res. Soc. Symp. Proc.* 851 (2005) 449–460.
- [29] P. Güthner, T. Ritter, K. Dransfeld, Temperature dependence of the piezoelectric constant of thin PVDF and P(VDF-TrFE) films, *Ferroelectrics* 127 (1992) 7–11.
- [30] N. Bassiri-Gharb, I. Fujii, E. Hong, S. Trolier-McKinstry, D.V. Taylor, D. Damjanovic, Domain wall contributions to the properties of piezoelectric thin films, *J. Electroceram.* 19 (2007) 49–67.
- [31] D.H. Reneker, A.L. Yarin, H. Fong, S. Koombhongse, Bending instability of electrically charged liquid jets of polymer solutions in electrospinning, *J. Appl. Phys.* 87 (2000) 4531–4547.

## Biographies

**Juan Pu** received her B.S. degree in electronic information engineering from University of Electronic Science and Technology of China (UESTC) in 2005. She has been pursuing her Ph.D. degree in optical engineering at UESTC since September 2005, and conducting research as a visiting student at UC-Berkeley since January 2009. Her current research interests include piezoelectric polymeric actuators, nanogenerators based on electrospun polymeric nanofibers and resonators.

**XiaoJun Yan** received his B.S. and Ph.D. degrees from Beihang University in 1995 and 2000, respectively. Since 2002, he has been a faculty member at Beihang University. Currently he is a professor in school of jet propulsion of Beihang University. His current research interests include structures of intellectual materials, high-temperature structural mechanics, piezoelectric actuator and self oscillator.

**Yadong Jiang** received his B.S., M.S. and Ph.D. degrees from University of Electronic Science and Technology of China (UESTC) in 1986, 1989 and 2001, respectively. After his graduation, he worked as a faculty member at UESTC. He is a professor in School of Optoelectronic Information of UESTC and the recipient of the special engaged professor of “Cheung Kang Scholar Program” and Distinguished Young Scholars of National Science Foundation of China. His current research interests include opto-electronic materials, organic materials, integrated devices, sensors and actuators.

**Chieh Chang** received his B.S. and M.S. degrees in power mechanical engineering from the National Tsing Hua University, Taiwan in 2001 and 2003 respectively, and Ph.D. degree in Mechanical Engineering from UC-Berkeley in 2009. Now he is a postdoctoral researcher at Sandia National Lab. His current research interests include nanomaterials synthesis and assembly, nanomaterials for energy conversion (energy harvesting and solar cells), nanomaterials for sensing and actuation, MEMS design, fabrication, packaging, and testing and piezoelectricity.

**Liwei Lin** joined UC-Berkeley in 1999 and is now chancellor's professor at the Mechanical Engineering Department and co-director at the Berkeley Sensor and Actuator Center. He received his B.S. (1986) in power mechanical engineering from National Tsing Hua University, M.S. (1991) and Ph.D. (1993) in mechanical engineering from the University of California at Berkeley. He was an associate professor in the Institute of Applied Mechanics, National Taiwan University, Taiwan (1994–1996) and an assistant professor in Mechanical Engineering Department, University of Michigan (1996–1999). His research interests are in design, modeling and fabrication of micro/nano-structures, micro/nano-sensors and micro/nano-actuators as well as mechanical issues in micro/nano-systems including heat transfer, solid/fluid mechanics and dynamics. Dr. Lin is the recipient of the 1998 NSF CAREER Award for research in MEMS Packaging and the 1999 ASME Journal of Heat Transfer best paper award for his work on micro-scale bubble formation. Currently, he serves as a subject editor for the IEEE/ASME Journal of Microelectromechanical Systems and the North and South America Editor of *Sensors and Actuators—A Physical*. He led the effort to establish the MEMS division in ASME and served as the founding Chairman of the Executive Committee from 2004 to 2005. He is an ASME Fellow and has 14 issued US patents in the area of MEMS.